Comparison of ATOVS, CHAMP and ground based humidity estimates on different spatiotemporal scales

J. Schulz[1], R. Lindau[2], N.Selbach[1], K.-B. Lauritsen[3], H. Gleisner[3]

[1]Deutscher Wetterdienst, Offenbach, Germany
[2]Meteorological Institute, University of Bonn, Germany
[3]Danish Meteorological Institute, Copenhagen, Denmark

Introduction

Humidity products can be derived from a large range of different satellite sensors including infrared and microwave sounders and imagers, VIS spectrometer and radio occultation instruments.
Within the Satellite Application Facility (SAF) on Climate Monitoring (CM-SAF), data from the SEVIRI instrument on the geostationary Meteosat satellite, the ATOVS infrared and microwave instrument suite onboard the polar-orbiting NOAA and future MetOp platforms, the IASI instrument on MetOp and the microwave radiometer SSM/I onboard DMSP platforms are used to develop a water vapor climatology. From its system version 3 onwards (operational in March 2007), CM-SAF will provide global estimates for individual instrument records.
The SAF on GRAS Meteorology (GRAS-SAF) is dedicated to radio occultation measurements from the EPS MetOp satellite, focusing on the Global Navigation Satellite Systems Radio Occultation Receiver for Atmospheric Sounding (GRAS) instrument. GRAS data is expected to improve on the traditional sounder products in the upper troposphere and lower stratosphere as well as under rainy conditions. Although the spatiotemporal sampling of the GRAS instrument is not as good as of other imagers or sounders, GRAS data can be used to construct an alternative single source climate product.

Objectives

The main objective of the joint visiting scientist activity of the GRAS-SAF and the CM-SAF is the investigation of the potential role of GRAS data within the humidity product suite of CM-SAF. Within this study, a comprehensive intercomparison of CHAMP, ATOVS, and ground based temperature and mixing ratio profiles in order to understand systematic differences between radio occultation and atmospheric sounder estimates better will be performed. The understanding of the systematic differences between water vapor estimates based on totally different measurement principles is considered to be a prerequisite for the application of merging algorithms to data from different instruments into a so-called best climate data set. ATOVS and CHAMP data are used to construct daily, monthly, and seasonal maps of integrated water vapor that are analyzed with respect to the different representation of spatial and temporal variability in the data sets. From this analysis it might be deducted on what spatiotemporal scales the individual estimates are best usable for the purpose of climate monitoring.

Retrieval and gridding technology

Table 1 gives an overview of the available products derived from ATOVS in the CM-SAF and the products derived at the GRAS-SAF. As visible in the table, the products are available on different spatial and temporal scales.

Table 1: Products from CM-SAF and GRAS-SAF

CM-SAF (ATOVS)	GRAS-SAF (GRAS)
Product Variables	
• Total precipitable water; • Temperature and mixing ratio profiles; • Vertically integrated precipitable water, vertically averaged relative humidity and temperature in 5 layers.	• Refractivity, “dry” variables; • Temperature, geopotential height, humidity profiles, surface pressure; • Vertically integrated variables.
Averaging Scales	
• Daily, monthly, seasonal, and annual mean; • Normal spatial resolution (60-90 km) gridded data; • Global data set.	• Monthly, seasonal, and annual mean; • Low spatial resolution (e.g. 10° lat/lon gridded data); • Global, hemispheric, and zonal data sets.

Products derived from ATOVS

Retrieval technique

The retrievals from ATOVS are based on the International ATOVS Processing package (IAPP) (Li et al., 2000). The processing package generates profiles of atmospheric temperature and moisture as well as different other atmospheric parameters. The most important parameters for the use in the humidity product of the CM-SAF are the temperature and moisture profiles. The retrieval can be applied to data of the National Oceanic and Atmospheric Administration 15 (NOAA-15) satellite and later data. However, due to a failure of the Advanced Microwave Sounding Unit A (AMSU-A) onboard the satellite NOAA-17, no retrievals can be done for this platform since the instrument has been switched off on Oct 30, 2003. The operational processing with the IAPP at CM-SAF employs numerical weather prediction (NWP) data as the only additional input to the retrieval in its current set up. The processing of IAPP uses the information from AMSU-A, AMSU-B and HIRS. The available Level 1d radiance files contain overlapping portions of individual NOAA orbits and are not matching the temporal output structure of the NWP model. Thus the level 1d radiances are reordered with respect to time in a way that they match the NWP data with a time window of ±1.5 hours around the model analysis time. DWD’s global GME model output is used as input to IAPP. The GME model has been chosen as input in order to be consistent with the other product groups of the CM-SAF. A detailed description of the global GME model principles can be found in Majewski et al. (2002). The analysis mode of the model is used as the input in IAPP. The initial retrieval results obtained from IAPP are quality checked with respect to, e.g., the minimum and maximum values of the calculated total precipitable water vapor (TPW). Temperature and humidity values for each of the retrieved pressure levels and each profile are checked for a valid range. Additionally, superadiabatic profiles are flagged. All retrievals failing at least one of the tests are flagged (i.e., set to a “no data” value) and not used in the further processing. From the ATOVS profiles, TPW and the layered precipitable water vapor (LPW) for 5 layers (1000-850, 850-700, 700-500, 500-300, 300-200 hPa) as well as mean temperatures and relative humidity for these layers are computed.

Gridding/Merging

A universally applicable technique to merge satellite data is used. It is based on the commonly known Kriging technique. The technique does not prescribe a fixed radius in which observations are considered at all, as performed in ordinary block Kriging. A more detailed description of the procedure is given in Lindau et al. (2004) and Lindau (2005). Our technique manages the aggregation

of additional information step by step, deciding at each stage which observation could contribute a maximum of new, not redundant information. This depends on the three characteristics of the potentially added observation: its distance to the predicting point, its individual error and its redundancy with the already aggregated observations.
Two pieces of information are necessary to run the Kriging procedure. These are (i) the spatial correlation function and (ii) the error of each observation. (i) The correlation function is derived to have an estimate how fast the reliability of an observation is decreasing with increasing distance. It is derived by fitting a quadratic exponential function to the data. Errors are definitely affecting the correlation function. However, it is shown that their impact can be easily corrected by a constant factor. (ii) The error variance of each individual observation is derived by decomposing the total variance at each grid point into an external and an internal part. For this purpose, daily averages for each 1° by 1° grid box are computed. The mutual variance of such averages is considered as external, the remaining variance within each of these boxes is regarded as internal. From the internal variance, the errors are concluded. However, the number of independent observations is crucial. Concerning satellite data, independence of pixels is a daring assumption. In fact, the analysis of variance revealed that only grid point averages of different satellites and/or instruments can be regarded as independent. In this context it should be mentioned that error covariance was not considered here. The Kriging procedure is used to combine the total and layered precipitable water fields and others derived from ATOVS instruments on different NOAA platforms.
It is an inherent benefit of Kriging to provide not only optimal interpolations, but also an error field for each map as additional benefit. However, it is exactly the knowledge of errors that makes the derived fields so valuable. Kriging is an interpolation scheme, i.e., it is able to predict values where no observation is available. The strength of Kriging lies in its ability to fill data gaps. Still, concerning ATOVS data, such data gaps remain rather limited, even on a daily basis, and could have been filled with much less effort.

Radio Occultation

A rather new method for the indirect measurement of temperature, pressure and water vapor in the stratosphere and the troposphere is based on atmospheric limb sounding by using the continuously broadcasted radio signals from the Global Navigation Satellite System (GNSS) satellites. The electron density in the ionosphere, the temperature, pressure and water vapor in the atmosphere influence these signals. The GNSS signals are delayed on the way through the ionosphere and atmosphere during the radio occultation. As a result, the ray path is slightly bent. This is observed in the amplitude and phase of the received signal on a Low-Earth Orbit (LEO) satellite “seeing” a GNSS satellite. Using inversion methods and geometrical considerations, the computation of a profile of the atmospheric refractivity at the position where the individual ray path has passed closest to the surface is possible if the position and velocity of the LEO and GNSS satellite are known. The refractivity is calculated using the Abel transform inversion method. The so-called “dry” temperature and pressure are obtained using the ideal gas law assuming hydrostatic equilibrium. Using ancillary data from an NWP model as temperature and humidity profiles as well as surface pressure being appropriate in time and location of the occultation, the temperature and humidity profiles are calculated in combination with the refractivity in a 1DVAR algorithm. A more detailed description of the principles can be found in, e.g., Wickert et al. (2004). As the radio occultation measurements are absolute, no calibration is needed. The observation geometry for one satellite leads to a global coverage of the products. One advantage of the radio occultation method is the high vertical resolution of the products and its insensitivity to clouds and rain.

Development of climatology

Several alternative techniques can be applied to construct climatological gridded fields. The chosen technique depends on the observational technique and the actual data set. Within the GRAS-SAF, three alternative methods for the construction of global climatologies from radio-occultation data have been investigated. These are relatively standard binning-and-averaging techniques, Bayesian fitting of global spherical harmonics to the observed radio occultation data, and 3D variational assimilation of the radio-occultation data into model fields. The first two methods, which are described in more detail below, can be used to generate true single-source climatologies. Unlike the assimilation approach, they do not depend on any other observational data than the radio-occultation profiles. The binning-and-averaging approach is also fully independent of any assumptions about the structure of the spatial distributions. The disadvantage of this independence from further underlying assumptions is, unfortunately, a lower spatial resolution. Using data from the GRAS/MetOp instrument alone, only the third approach can give something close to a high spatial resolution.

In preparation of the EUMETSAT MetOp mission, a straight-forward method of averaging into equal-angle grid boxes has been studied, In the absence of actual observations, "observed" data have been obtained by sampling a climate model data set, e.g., the ERA-40 re-analysis, at the locations of the simulated GRAS/MetOp observations. All "observations" falling within a grid box and within a suitable averaging time interval, e.g., 1 month, 3 months or a year, are averaged into a climate variable. The resulting "observed" average can then be compared with the corresponding "true" average, thus revealing any errors, e.g., the effects if under-sampling. The intention is to use this method in the future to simulate sampling errors and the effects of observational errors on climate data derived from actual observations.

Fitting a global function, such as a series of spherical harmonics, to all data retrieved at a certain pressure level during a suitable averaging interval, e.g., one month, is an alternative method:

$$Y(\lambda,\mu) = \sum_{k=1}^{Ncoef} w_k \phi_k(\lambda,\mu)$$

Here λ and μ are the longitude and latitude, while ϕ_k is a spherical-harmonic term evaluated at the observed locations. The weights w_k are found through an extended least chi-squared fit to the observed data, subject to a smoothness condition:

$$M(w,\alpha,\beta) = \frac{\beta}{2}(\bar{y} - \mathbf{\Phi}\bar{w})^T(\bar{y} - \mathbf{\Phi}\bar{w}) + \frac{\alpha}{2}\bar{w}^T\mathbf{C}\bar{w}$$

where β is related to the variability of the observations with respect to the fit, and α is a measure of the smoothness of the fit. Using the bayesian principles described in Leroy (1997), and further explored in Haan (2005). optimal values of w, α, β and the number of spherical-harmonics terms can be found simultaneously in order to avoid over-fitting the data. A decisive advantage of this method is that no information on observation error correlations or background error correlations is required. The final products are the actual fit in a spectral form and an estimate of the uncertainty of the fit. The latter is solely related to the fit itself but may nevertheless be used to reveal problems with the data.

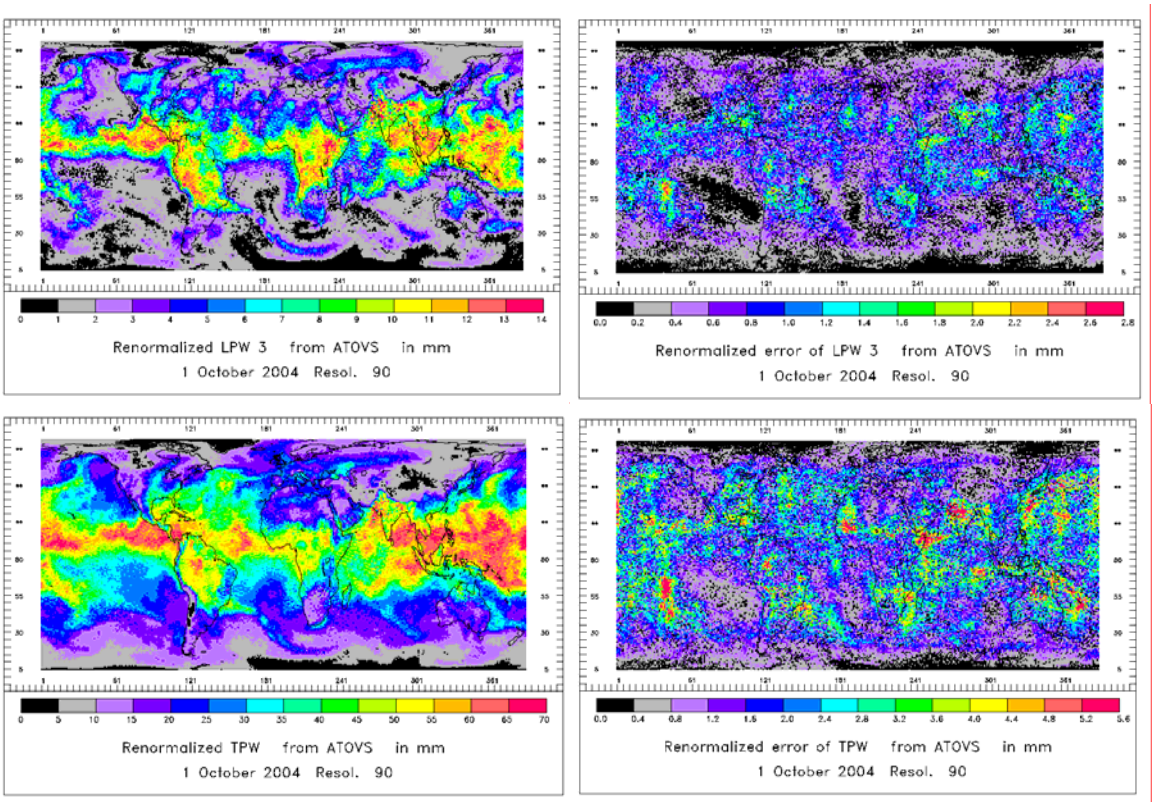

Fig. 1: Example of daily mean for 1 October 2004 from ATOVS for layered precipitable water from 700 hPa – 500 hPa (upper left) and TPW (lower left) and the corresponding standard deviations (upper and lower right)

Within the CM-SAF, fields are constructed by applying a Kriging scheme that was adjusted for the use with satellite data to derive daily averages. Fig. 1 shows CM-SAF daily products for precipitable water in 2 layers the atmosphere together with the corresponding error estimates. Fig. 2 shows a typical GRAS-SAF global map of monthly mean 200 hPa geopotential height (left panel) and the corresponding error map (right panel) obtained from data of the research satellite CHAMP (Wickert et al, 2001, Reigber et al, 2002,2005) . Around 4000 samples have been used. The global maps are created by fitting spherical harmonics to the radio occultation data. The fittings are constrained by Bayesian principles.

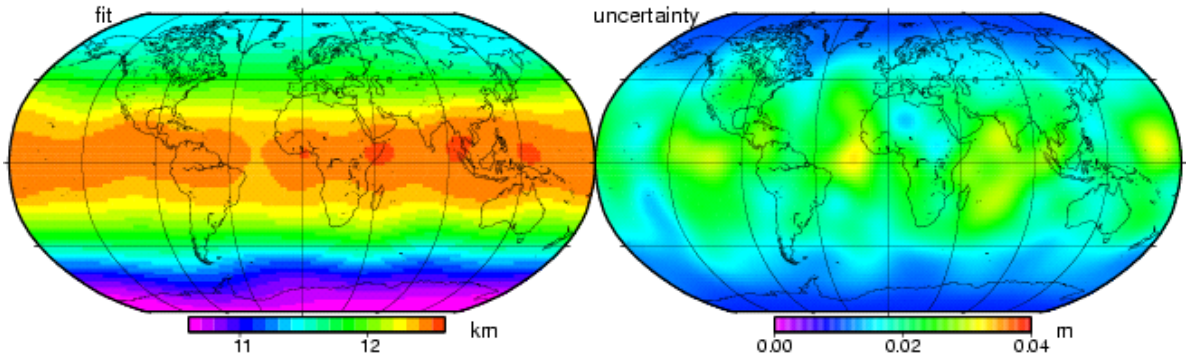

Fig. 2: Bayesian fitting of global spherical harmonics to data from CHAMP. The figure shows the monthly mean (left) and uncertainty of fit (right) of the 200 hPa geopotential height.

The four pictures in Fig. 1 show middle layer 700-500 hPa (top right) and total (bottom right) vertically integrated precipitable water at 1 October 2004 derived from individual ATOVS soundings employing a Kriging algorithm. The basic temperature and moisture profiles are retrieved using the IAPP retrieval package. Figures in the left column show the daily mean value, figures in the right show the Kriging error that represents the sampling error as no retrieval error information is given for the IAPP retrieval.

Validation of products from ATOVS versus ground based data

Independent ground based temperature and water vapor measurements are needed to assess the quality of the retrieval schemes and derived products. Data from operational radiosonde networks, ground-based global positioning system (GPS) measurements and dedicated reference sites will be used to assess the quality of the derived CM- and GRAS-SAF products. Reference site data are available from the three fixed ARM sites in Alaska (USA), Oklahoma (USA), and Nauru (Fidji) and the DWD site at Lindenberg (Germany). Additionally, a mobile ARM facility has been placed in North-West Africa during 2006. Those sites provide for instance lidar and microwave profiler measurements with high temporal resolution that enables direct matching of individual satellite retrievals. Radiosondes from the Global Upper Air Network (GUAN) can be used to assess the quality of spatiotemporal averaged products.

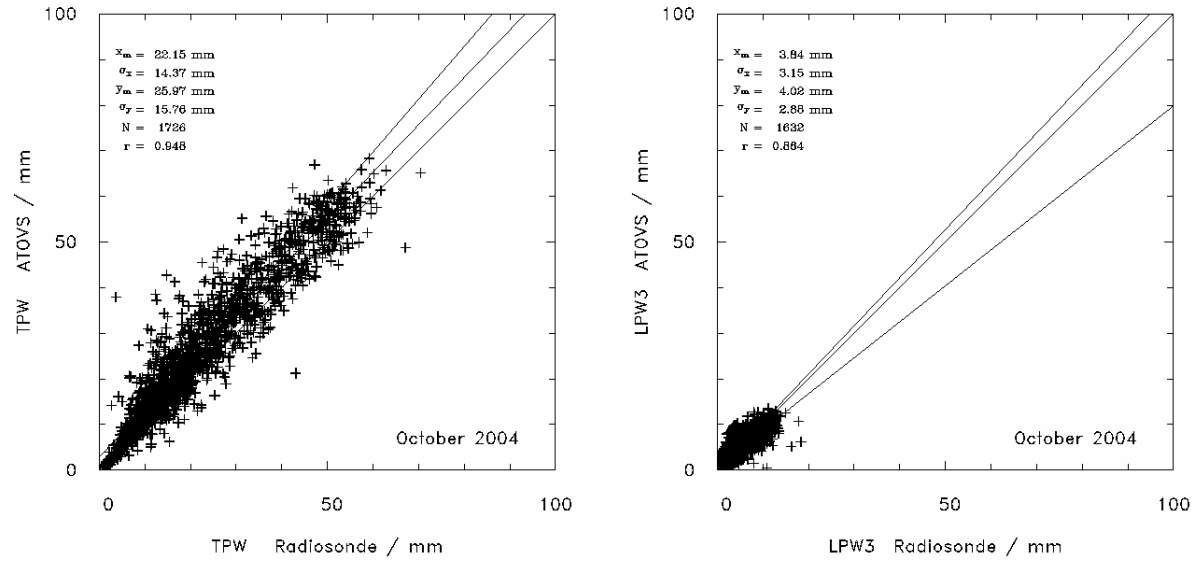

Fig 3: Comparison of TPW (left) and LPW (700 hPa – 500 hPa) (right) from ATOVS and radiosonde profiles

Fig. 3 shows a preliminary comparison of daily means of total column precipitable water (left) and a layer between 700 hPa and 500 hPa over land derived from ATOVS to GUAN radiosondes for October 2004. After applying the Kriging routine to ATOVS data, the output represents averages over 90 km by 90 km in space and 24 hours, whereas radiosondes can be regarded as point measurements. In order to account for the difference in temporal resolution, the radiosonde data is averaged over one day. Only days providing at least two ascents are taken into account. The mean spatial variance of daily means within a box of 90 km by 90 km is missing in the ATOVS data. Lindau and Ruprecht (2000) estimated the variance of TPW on different temporal and spatial scales from GPS measurements and found a mean temporal variance of TPW within one day of about 8 mm². The

Table 2: Summary of bias and correlation (r) statistic for the comparison of the layered and total precipitable water vapor from ATOVS and radiosonde data.

Month	Total			1000-850 hPa			850-700 hPa			700-500 hPa			500-300 hPa			300-200hPa		
	Bias		r	Bias		r	Bias		r	Bias		r	Bias		r	**Bias**		**r**
	mm	%	-	mm	%	-	mm	%	-	mm	%	-	mm	%	-	mm	**%**	**-**
10/04	3.82	17	0.95	2.35	21	0.96	0.73	11	0.91	0.18	5	0.86	0.0	0	0.77	0.19	211	0.45
11/04	3.34	16	0.96	2.10	20	0.97	0.53	9	0.93	0.10	3	0.88	-0.03	-3	0.80	0.17	18	0.46
12/05	3.63	19	0.96	2.13	22	0.97	0.75	13	0.93	0.11	3	0.90	0.0	0	0.85	0.15	166	0.54
01/05	3.85	20	0.96	2.23	24	0.97	0.74	13	0.94	0.19	5	0.90	-0.01	-1	0.88	0.15	166	0.58
02/05	3.94	19	0.95	2.19	22	0.97	0.75	12	0.93	0.22	6	0.89	0.0	0	0.86	0.15	150	0.39
03/05	3.20	16	0.96	1.98	20	0.97	0.61	10	0.93	0.06	2	0.90	-0.01	-1	0.84	0.13	118	0.41
04/05	3.33	16	0.94	2.05	20	0.95	0.48	8	0.93	0.12	3	0.88	-0.03	-3	0.83	0.14	127	0.52
05/05	3.51	15	0.94	2.12	19	0.95	0.64	9	0.90	0.10	2	0.88	-0.07	-5	0.80	0.21	175	0.51
06/05	4.23	16	0.95	2.67	21	0.95	0.83	10	0.92	0.21	4	0.90	-0.02	-1	0.86	0.25	192	0.54
07/05	4.59	16	0.95	3.11	22	0.93	0.91	10	0.92	0.11	2	0.89	-0.06	-4	0.87	0.26	186	0.52

spatial variance on a scale of 90 km was found to be 3 mm². The study was based on individual measurements, thus a value of 3 mm² is the upper limit of the variability of daily mean values. Their variance should be lower than the one of high resolution data. The magnitude of missing spatial variance (0 – 3 mm) within ATOVS data is small compared to the total variance considered in Fig.3 (225 mm^2, corresponding to a standard deviation of about 15 mm), so that this effect can be neglected. The comparisons have been done for the period October 2004 to July 2005. The total precipitable water from ATOVS has a ~10% bias introduced in the near surface layer whereas for the middle tropospheric layer the bias is only around 1.5-5%. The near surface bias is most likely be introduced by NWP model information (German global model in this case). This is used as a first guess and it is not much changed over land surfaces due to limited water vapor information from HIRS in the lower atmosphere. Table 2 shows the bias, given as absolute value (ATOVS – radiosonde) and in percent (relative to radiosonde) as well as the correlation statistic for each month in the period October 2004 to July 2005. As can be seen from Table 2, the values do not vary much within this time period. The relative bias is high in the lower atmospheric layers (1000 hPa – 850 hPa, 850 hPa – 700 hPa), while it is much lower in the upper tropospheric layers, with values in the range of 3 % for the layer between 700 hPa and 500 hPa and about -1.5 % for the layer 500 hPa – 300 hPa, respectively. The interpretation of the most upper layer is difficult as the amount of integrated water vapor is already very small in these heights of the atmosphere and small absolute errors already result in high relative errors. However, one may say that the bias is positive. This is consistent with the dry bias that radiosondes tend to have at this height (John and Buehler, 2005). The bias in the total water vapor is dominated by the bias in the two lowest layers of the integrated water vapor product. This is due to the exponential structure of the water vapor profile. A more detailed description of the validation of the products derived from ATOVS is given in Schulz (2006). First tests have been performed in order to check for the source of the bias in TPW compared to the radiosondes. The validation data set for October 2004 has been divided into several classes in order to investigate the influence of the ice and snow-covered Antarctic region, the effect of high orography as well as the difference in the performance of the IAPP retrieval over land and open water. A similar bias has been found for these cases. Additional studies will be performed using different NWP data as input to check the influence of the auxiliary input on the retrieval results and, therefore, on the products calculated for CM-SAF.

References

Haan, S. de, 2005: Global Maps from GPS Radio Occultation Data, *DMI Scientific Report 05-08*, DMI, Copenhagen, 52 pp.

John, V. O., S. A. Buehler, 2005: Comparison of microwave satellite humidity data and radiosonde profiles: A survey of European stations, *Atmos. Chem. Phys.*, **5**, 1843-1853.

Leroy, S,. 1997: Measurement of geopotential heights by GPS radio occultation, *J. Geophys. Res.*, **102**, 6971-6986.

Li, J., W. W. Wolf, W. P. Menzel, W. Zhang, H.-L. Huang, and T. H. Achtor, 2000: Global soundings of the atmosphere from ATOVS measurements: The algorithm and validation. *J. Appl. Meteor.*, **39**, 1248-1268.

Lindau, R. and J. Schulz, 2004: Gridding/merging techniques for the humidity composite product of the CM-SAF. *Proceedings of the 2004 EUMETSAT Meteorological Satellite Conference, Prague, Czech Republic*, EUM P41, 519-526.

Lindau, R., 2005: Optimal Merging of water vapour retrievals from different instruments (OMDI), *Visiting Scientist Report*, DWD, 33pp.

Lindau, R. and E. Ruprecht, 2000: SSM/I-derived total vapour content over the Baltic Sea compared to independent data, *Met. Zeitschrift*, **9**, No.2, 117-123.

Majewski D., D. Liermann, P. Prohl, B. Ritter, M. Buchhold, T. Hanisch, G. Paul, W. Wergen, and J. Baumgardner, 2002: The operational global icosahedral-hexagon grid point model GME: description and high resolution tests, *Mon. Wea. Rev.*, **130**, 319-338.

Reigber, C., H. Lühr, and P. Schwintzer, 2002: CHAMP mission status, *Adv. Space Res.*, **30**(2), 129– 134.

Reigber, C., H. Lühr, P. Schwintzer, and J. Wickert, 2005: *Earth Observation With CHAMP: Results From Three Years in Orbit*, Springer, New York, 628 pp.

Schulz, J., 2006: On the Validation of the Humidity Composite Product (CM-SAF version 3), SAF/CM/DWD/SR/HCP/3, Issue 1.0, 73 pp.

Wickert,, J., C. Reigber, G. Beyerle, R. Koenig, C. Marquardt, T. Schmidt, L. Grunwaldt, R. Galas, T. K. Meehan, W. G. Melbourne, and K. Hocke, 2001: Atmosphere sounding by GPS radio occultation: First results from CHAMP, *Geophys. Res. Lett.*, **28**(17), 3263–3266.

Wickert, J., T. Schmidt, G.Beyerle, R.König, C.Reigber and N. Jakowski, 2004: The Radio Occultation Experiment aboard CHAMP: Operational Data Analysis and Validation of Vertical Atmospheric Profiles. *J. Meteorol. Soc. Jpn.*, **82**, 381-395.